

The Structure of Clusters with Bimodal Distributions of Galaxy Radial Velocities. I. A1035

A. I. Kopylov¹ and F. G. Kopylova¹

¹*Special Astrophysical Observatory of the Russian AS, Nizhnij Arkhyz 369167, Russia*

(Received July 9, 2007; Revised July 19, 2007)

The structure of the A1035 cluster of galaxies ($10^h32^m+40^013'$, $cz \sim 22000 \text{ km s}^{-1}$), which exhibits a bimodal distribution of galaxy radial velocities ($\Delta V \approx 3000 \text{ km s}^{-1}$), is analyzed using three methods of determining the relative distances to clusters from early-type galaxies: the Kormendy relation corrected for the dependence of residuals on galaxy magnitude, the photometric plane, and the fundamental plane. We use the data obtained with the 1-m telescope of the Special Astrophysical Observatory of the Russian Academy of Sciences and SDSS (DR5) data to show that A1035 consists of two gravitationally unbound independent clusters. These clusters with the velocity dispersions of 566 km s^{-1} and 610 km s^{-1} and masses within R_{200} equal to $2.7 \cdot 10^{14}$ and $3.5 \cdot 10^{14} M_{\odot}$, respectively, obey the Hubble law.

1. INTRODUCTION

Different methods of determination of masses of clusters of galaxies (based on x-ray flux, gravitational lensing of galaxies by the cluster, or on the virial theorem) yield the results that agree well with each other for the central regions of regular clusters. The mass distribution on scale lengths exceeding the size of virialized cluster regions (1–2 Mpc) is much more poorly known. In this connection it is of interest to study the dynamics of interaction of neighboring clusters and subclusters within the same cluster. The velocity dispersion amounts to $1000 - 1500 \text{ km s}^{-1}$ in the richest clusters, where galaxies sometime form complex structures — subclusters. Of special interest are the cases where the velocity distribution in a cluster has a bimodal form. A $3000 - 3500 \text{ km s}^{-1}$ difference between the mean radial velocities may be due to either the gravitational interaction between extremely massive clusters colliding close to the line of sight (see Hayashi and White[1] for theoretical estimates of limiting velocities in terms of the Λ CDM), or to the line-of-sight projection of unbound clusters.

Sufficiently reliable direct estimates of the distances to subclusters have been obtained for two clusters with a bimodal galaxy velocity distribution: A3526 (Centaurus) [2] and A2626 [3]. In both cases the subclusters are located at the same heliocentric distance and the velocity difference (1500 and 2600 km s^{-1} , respectively) is due to the gravitational interaction between the subclusters. In

Table 1. Parameters of early-type galaxies based on the results of observations made with the 1-m telescope

Cluster	Galaxy No.	α (J2000) δ	z_h	cz_h , km s ⁻¹	m_R , mag	R_e , arcsec	μ_e , mag/□''	n
A1035A	1	10 32 23.47 +40 10 08.6	0.067020	20092	14.15	10.33	22.61	1.92 ± 0.46
A1035A	2	10 32 15.27 +40 10 12.5	0.067040	20098	14.30	14.06	23.38	4.95 ± 1.26
A1035A	3	10 32 28.89 +40 08 54.6	0.068691	20593	14.82	4.55	21.26	1.29 ± 0.19
A1035A	4	10 31 55.98 +40 06 43.7	0.068831	20635	14.99	3.09	20.45	2.52 ± 1.64
A1035A	5	10 32 05.95 +40 17 25.7	0.072430	21714	15.20	3.84	21.36	2.07 ± 0.24
A1035A	6	10 32 12.49 +40 08 08.4	0.065940	19768	15.55	3.60	21.48	1.52 ± 0.15
A1035A	7	10 32 19.90 +40 08 26.5	0.065582	19661	15.50	3.27	21.25	2.48 ± 0.54
A1035A	8	10 31 37.06 +40 07 39.6	0.071793	21523	15.70	2.94	21.14	1.88 ± 1.93
A1035A	9	10 31 22.79 +40 10 09.9	0.068496	20535	16.08	2.24	20.89	1.15 ± 0.11
A1035B	1	10 32 13.92 +40 16 16.4	0.077816	23329	13.77	11.64	22.51	4.91 ± 0.71
A1035B	2	10 31 57.03 +40 18 20.7	0.078951	23669	15.22	3.96	21.59	3.67 ± 0.43
A1035B	3	10 32 07.42 +40 10 30.3	0.076860	23042	15.42	4.06	21.54	2.48 ± 0.51
A1035B	4	10 32 10.77 +40 17 02.4	0.081590	24460	16.02	2.77	21.34	2.50 ± 1.51
A1035B	5	10 31 37.75 +40 10 32.6	0.077238	23155	16.17	2.72	21.49	1.34 ± 0.62
A1035B	6	10 32 07.52 +40 15 49.7	0.074700	22394	16.44	2.21	20.99	—
A1035B	7	10 32 18.29 +40 17 01.5	0.078633	23574	16.43	3.16	21.90	0.91 ± 0.45

the case of A2626 the higher subcluster velocity difference compared to velocities of internal motions may be due to the large mass of the (dark) matter at the periphery of the clusters [3].

We selected a total of four rich clusters (A1035, A1569, A1775, and A1831) with a bimodal distributions of galaxy radial velocities ($\Delta V \sim 3000$ km s⁻¹) for direct (i.e., redshift independent) determination of subcluster distances and for the determination of the nature of interaction between the subclusters. In this paper we determine the (line-of-sight) structure of the A1035 cluster using three different methods to estimate relative distances from early-type galaxies. This work makes use of observational material obtained with the 1-m telescope of the Special Astrophysical Observatory of the Russian Academy of Sciences and the data of the SDSS (Sloan Digital Sky Survey) catalog.

This paper has the following layout. Section I gives an introduction. Section II describes samples of early-type galaxies. Section III describes the specifics of the use of samples for the determination of distances to clusters of galaxies and their analysis. In conclusion, we list the main results of this study. We adopt the following values for cosmological parameters: $\Omega_m = 0.3$, $\Omega_\Lambda = 0.7$, and $H_0 = 70$ km s⁻¹ Mpc⁻¹.

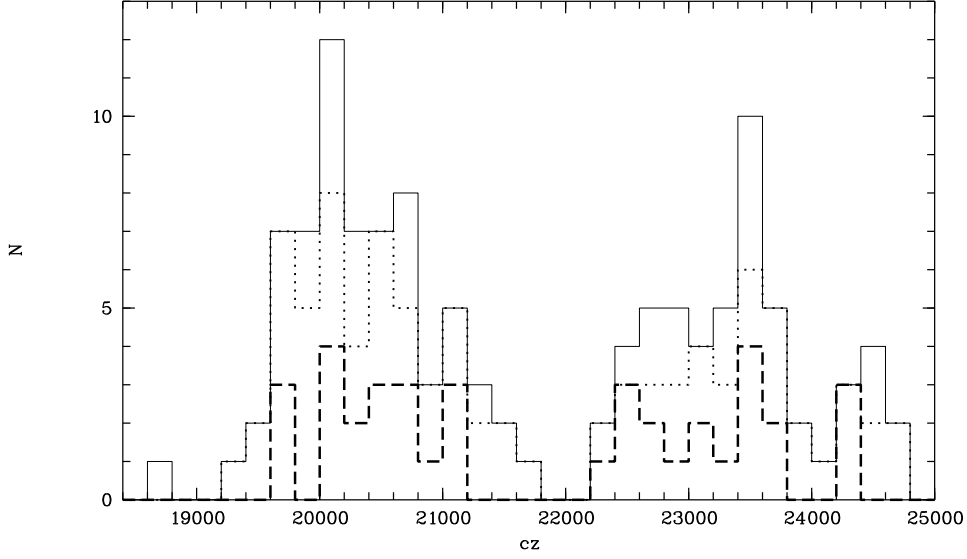


Figure 1. Distribution of galaxy radial velocities in the A1035 cluster inside the $30'$ (the solid line) and inside the R_{200} (the dotted line) clustercentric radius. The dashed line shows the distribution of early-type galaxies inside R_{200} .

2. DESCRIPTION OF DATA

In this section we describe observational data — the parameters of early-type galaxies that we use to determine the relative distances to the subsystems in the A1035 cluster [4]. According to Abell’s catalog, this cluster has a radial velocity of $cz \simeq 24000$ km/s, richness class 2, and belongs to Bautz-Morgan II–III type. We use SDSS (DR5) data to identify two subsystems — A1035A and A1035B — in the A1035 cluster (Fig. 1 shows the velocity distribution). Figures 2 and 3 show our results for the main parameters of the clusters: deviations of the radial velocities of cluster members from the mean radial velocity of the cluster; integrated distribution of clustercentric distances of cluster members, and the sky-plane locations of cluster members. The center of A1035B coincides with the position of the brightest cD galaxy and with the peak of x-ray flux distribution. We adopt the center of A1035A to be located between the two brightest galaxies.

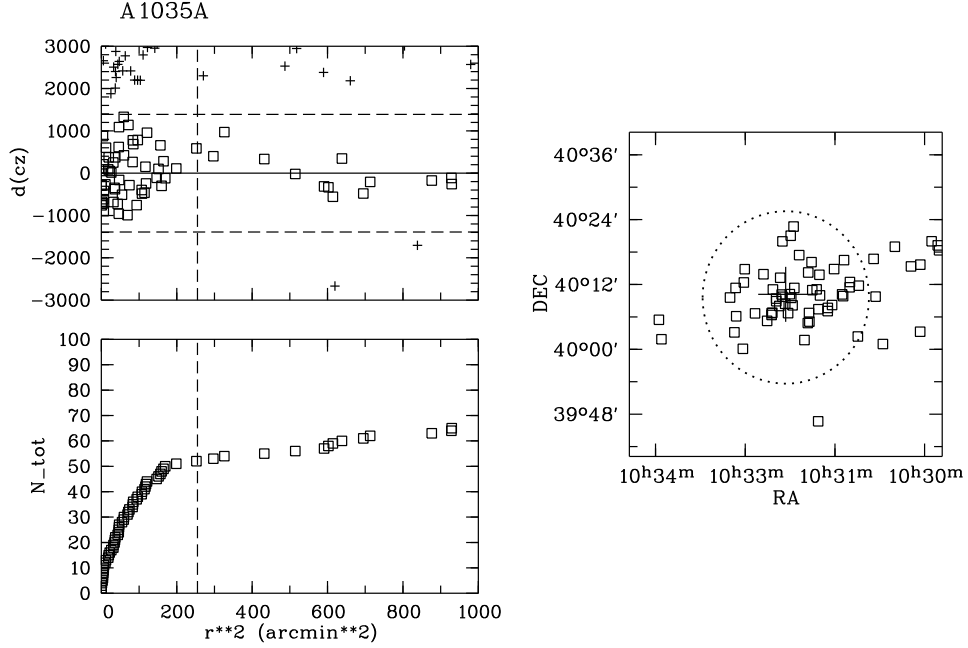


Figure 2. Distribution of galaxies in A1035A. The top left panel shows the deviation of galaxy radial velocities from the mean radial velocity: the dashed lines correspond to the $\pm 2.5\sigma$ deviation and the vertical dashed line corresponds to the R_{200} radius. The squares and plus signs indicate cluster members and field galaxies, respectively. The bottom left panel shows the integrated distribution of the number of galaxies as a function of squared clustercentric angular distance. The same designations are used. The right-hand panel shows the sky-plane distribution of cluster galaxies. The circle shows the R_{200} -radius region in arcmin. The cross indicates the cluster center.

Table 2. Parameters of early-type SDSS galaxies

Cluster.	α ($J2000$)	δ	z_h	cz_h , km s $^{-1}$	σ , km s $^{-1}$	r , mag	R_e , arcsec	$fracDeV_r$	$r90/r50$	$eClass$
A1035A	10 32 15.27	+40 10 12.5	0.067102	20117	208	15.18	4.24	1.000	3.49	-0.159
A1035A	10 32 28.89	+40 08 54.6	0.066943	20069	196	15.22	5.34	0.907	2.93	-0.142
A1035A	10 32 23.47	+40 10 08.6	0.066900	20056	220	15.26	4.47	1.000	3.38	-0.162
A1035A	10 31 55.98	+40 06 43.7	0.069003	20687	240	15.30	3.05	0.980	3.11	-0.143
A1035A	10 32 33.51	+40 06 41.6	0.069241	20758	199	15.52	3.65	1.000	3.28	-0.132
A1035A	10 32 12.49	+40 08 08.4	0.065940	19768	177	15.80	4.24	0.952	3.18	-0.137
A1035A	10 32 19.90	+40 08 26.5	0.065582	19661	208	15.85	2.80	1.000	3.17	-0.142
A1035A	10 33 00.49	+40 14 50.3	0.070582	21160	163	16.14	2.85	1.000	3.26	-0.122
A1035A	10 31 52.75	+40 10 56.7	0.068040	20398	190	16.18	2.78	0.918	2.90	-0.156
A1035A	10 32 24.94	+40 13 14.6	0.067106	20118	148	16.33	3.06	0.904	3.02	-0.140

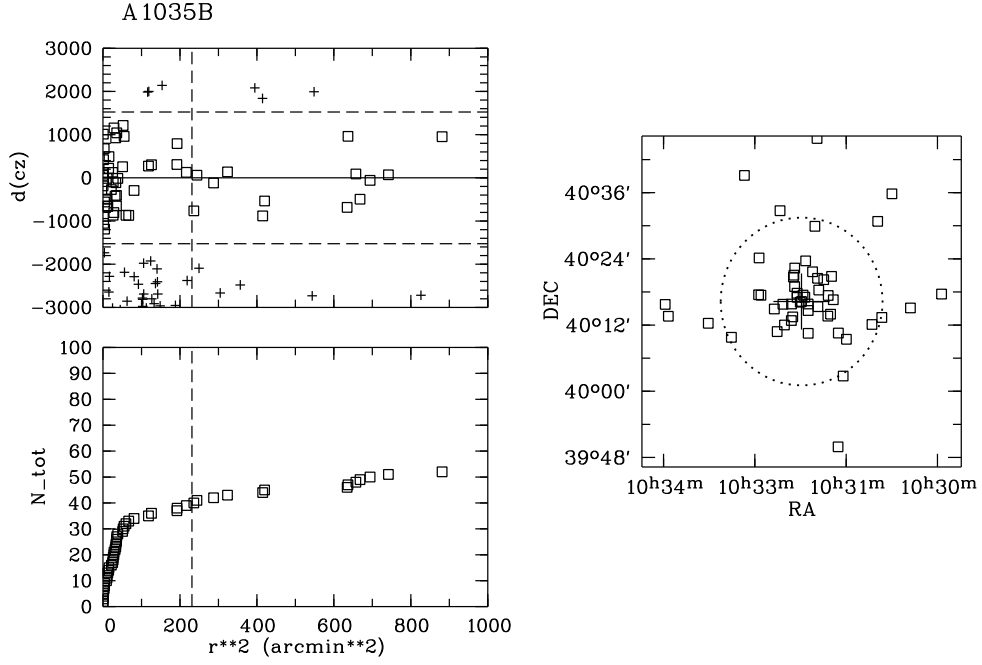


Figure 3. Same as Fig. 2, but for A1035B.

Table 2. (Contd.)

Cluster	α (J2000)	δ	z_h	cz_h , km s ⁻¹	σ , km s ⁻¹	r , mag	R_e , arcsec	$fracDeV_r$	$r90/r50$	$eClass$
A1035A	10 32 22.64	+40 19 58.5	0.070606	21167	129	16.36	2.82	1.000	2.62	-0.152
A1035A	10 31 22.79	+40 10 09.9	0.068496	20535	164	16.42	1.50	1.000	2.99	-0.136
A1035A	10 31 56.77	+40 14 12.7	0.067393	20204	124	16.46	2.74	0.859	2.88	-0.129
A1035A	10 31 14.93	+40 12 26.9	0.070187	21042	125	16.54	2.15	1.000	3.12	-0.126
A1035A	10 32 17.02	+40 06 42.1	0.070001	20986	132	16.95	2.17	1.000	2.91	-0.128
A1035A	10 31 20.88	+40 16 30.6	0.068932	20665	115	16.96	1.73	0.906	2.73	-0.123
A1035A	10 31 45.59	+40 13 47.7	0.065967	19776	147	17.07	1.74	0.908	2.84	-0.150
A1035A	10 32 33.59	+40 06 21.4	0.068162	20434	114	17.10	2.72	0.831	2.83	-0.125
A1035A	10 31 06.04	+40 11 46.5	0.068363	20495	151	17.15	1.36	0.978	2.72	-0.132
A1035B	10 31 57.03	+40 18 20.7	0.079322	23780	218	15.56	4.25	1.000	3.31	-0.143
A1035B	10 31 04.63	+40 12 06.9	0.080857	24240	146	15.84	4.89	1.000	2.95	-0.140
A1035B	10 32 54.02	+40 17 24.3	0.075323	22581	219	16.31	1.85	1.000	3.34	-0.134
A1035B	10 32 10.77	+40 17 02.4	0.081375	24396	153	16.33	3.20	0.848	2.93	-0.128
A1035B	10 31 47.68	+40 17 21.7	0.075329	22583	170	16.36	3.17	1.000	2.94	-0.157
A1035B	10 31 48.12	+40 13 36.7	0.076802	23025	134	16.45	2.00	1.000	3.01	-0.138
A1035B	10 32 18.29	+40 17 01.5	0.078633	23574	121	16.71	3.36	0.997	2.64	-0.137

Table 2. (Contd.)

Cluster	α (J2000) δ	z_h	cz_h , km s ⁻¹	σ , km s ⁻¹	r , mag	R_e , arcsec	$fracDeV_r$	$r90/r50$	$eClass$
A1035B	10 32 07.52 +40 15 49.7	0.074700	22394	195	16.74	2.12	0.817	2.68	-0.136
A1035B	10 32 22.67 +40 13 28.5	0.078169	23434	159	16.92	1.39	1.000	2.98	-0.126
A1035B	10 33 23.12 +40 09 46.5	0.078639	23575	141	16.97	1.93	1.000	2.83	-0.112
A1035B	10 32 56.32 +40 17 29.7	0.075317	22579	153	17.02	1.21	1.000	3.04	-0.124
A1035B	10 31 52.13 +40 20 13.4	0.081302	24374	122	17.10	3.44	0.974	2.82	-0.106
A1035B	10 32 20.82 +40 18 58.5	0.076050	22799	122	17.17	2.00	0.831	2.67	-0.137
A1035B	10 31 58.21 +40 20 28.3	0.077899	23354	145	17.44	1.40	0.947	2.69	-0.136
A1035B	10 32 22.02 +40 20 40.8	0.077310	23177	114	17.45	1.41	0.964	2.66	-0.097
A1035B	10 32 38.02 +40 10 48.7	0.079071	23705	139	17.45	1.74	1.000	2.72	-0.099
A1035B	10 32 21.50 +40 21 02.7	0.078636	23574	102	17.47	1.52	1.000	2.93	-0.021
A1035B	10 32 23.81 +40 15 49.0	0.076353	22890	151	17.47	1.54	1.000	3.03	-0.111
A1035B	10 32 40.81 +40 14 55.0	0.075532	22644	117	17.69	1.28	0.909	2.77	-0.104

Table 3 lists the cluster parameters that we determined for the objects located within the R_{200} radius according to SDSS data. Here R_{200} is the radius of the virialized part of the cluster where the mass density exceeds the critical density of the Universe by a factor of 200. In this case, the cluster mass can be determined from R_{200} and velocity dispersion σ . We determined the average radial velocity cz of the cluster and its dispersion σ iteratively: we first use all galaxies with measured radial velocities ($N = 65$ and $N = 52$ in A1035A and A1035B, respectively) inside the region of radius $30'$ studied here except for those that deviate by more than 2.5σ . We further assume that the clusters are in virial equilibrium and that their masses increase linearly with radius to compute, with the resulting velocity dispersion, the radius $R_{200} = \sqrt{3}\sigma(1+z)^{-3/2}/(10H_0)$ Mpc [5] and redetermine the average cluster radial velocity cz and its dispersion σ_{200} inside the R_{200} radius. The virial mass within this radius is equal to $M_{vir,200} = 3G^{-1}R_{200}\sigma_{200}^2$. Here N_{200} is the number of galaxies with measured radial velocities located inside R_{200} . We adopt the x-ray luminosities from Rines and Diaferio [6]. The same authors showed that A1035 consists of two subclusters. Figure 1 shows the distribution of galaxy radial velocities in the systems inside the selected radius.

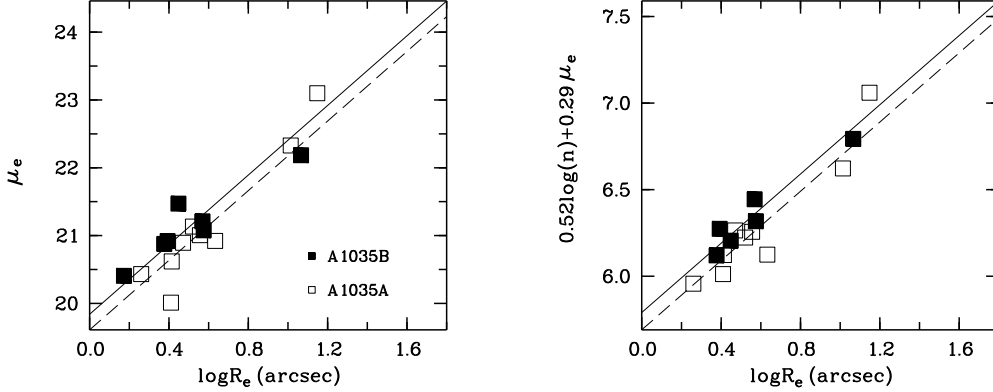


Figure 4. The Kormendy relation (the left-hand panel) and photometric plane (the right-hand panel) for early-type galaxies in A1035A and A1035B based on the results of observations made with the 1-m telescope. The dashed and solid lines indicate the zero points of clusters A and B, respectively.

Table 3. Cluster data

Cluster	α (J2000)	δ	z_h	cz_h , km s $^{-1}$	σ , km s $^{-1}$	R_{200} , Mpc	N_{200}	M_{200} , $10^{14} M_{\odot}$	L_x , 10^{43} erg s $^{-1}$
A1035A	10 32 19.36	+40 10 10.4	0.067992	20383	556 ± 77	1.24	52	2.68 ± 0.74	0.7
A1035B	10 32 13.95	+40 16 16.5	0.078216	23448	610 ± 98	1.35	39	3.52 ± 1.13	2.0

2.1. The Data for Early-Type Galaxies Based on Observations Made with the 1-m Telescope

The relative distances of clusters of galaxies in sufficiently distant regions with $z = 0.05$ and higher are determined using parameters of early-type galaxies (e.g., [7]; [8]). In this paper we use three methods based on the properties of early-type galaxies to estimate the peculiar motions of clusters A1035A and A1035B: the Kormendy relation [9], the photometric plane (PhP) [10], and the fundamental plane (FP) [11]. To accomplish our task, we determined the parameters of 16 galaxies in the systems studied using the direct R_c -band (the Kron–Cousins system) images that we took

with the 1-m telescope of the Special Astrophysical Observatory of the Russian Academy of Sciences in 1998, 1999, and 2003 under average seeing conditions ($1.5''$) measured as the FWHM of a star's profile. In 1998 and 1999 a 520×580 ISD015A CCD was used with a pixel size of $18 \times 24 \mu\text{m}$, which corresponds to an angular size of $0.28'' \times 0.37''$. In 2003, a 2048×2048 CCD with an angular pixel size of $0.43''$ was used. The exposures were equal to 500 or 600 s. Landolt's [12] standard stars were observed several times during each night to provide photometric calibration.

We use MIDAS (Munich Image Data Analysis System, [13]) to reduce the observational data. We apply the standard procedure of image reduction: subtraction of median dark frame, division by flat field, and subtraction of the sky background approximated by a quadric surface. We use multiaperture photometry to determine the total asymptotic magnitude of each galaxy. We then use the total magnitude to determine the effective radius R_e of the circle where the galaxy luminosity decreases by a factor of two, and the effective surface brightness μ_e at this radius. We determine the exponent n characterizing the shape of the surface brightness profile by fitting a Sersic [14] profile $R^{1/n}$ ($n = 4$ for the de Vaucouleurs [15] profile) to the observed profile in the galactocentric radius interval from 3 FWHM out to the radius where the surface brightness equals $24^m - 25^m \text{ arcsec}^{-2}$. We then use the method proposed by Saglia et al. [16] to correct the resulting photometric parameters of galaxies (R_e and μ_e), except for n . We compare independent measurements for 15 galaxies that we observed twice to find that the standard error of measured μ_e and $\log(R_e)$ is equal to $0.^m09$ and 0.02 , respectively. We thus use model-independent galaxy parameters (R_e , μ_e) estimated from the total asymptotic absolute magnitude, and model-dependent quantity n . The asymptotic magnitude was difficult to determine for the three brightest galaxies (of very large size), and that is why we estimate all parameters by fitting Sersic's profile to observations.

Table 1 features the results of our photometric measurements. It contains the following data (the observed galaxy parameters are not corrected for seeing): the number of the cluster according to Abell's catalog; the number of the galaxy; the J2000 equatorial coordinates of galaxies; the heliocentric redshift and radial velocity (according to NED); the total (asymptotic) magnitude; the effective radius of the galaxy in arcseconds; the effective surface brightness at the effective radius, and the Sersic profile shape parameter n and its error.

2.2. Data for Early-type Galaxies from the SDSS Catalog

We compiled a sample of early-type galaxies in the A1035A and A1035B clusters based on SDSS DR5 [17] data (r -band). We selected galaxies based on the criteria proposed by Bernardi

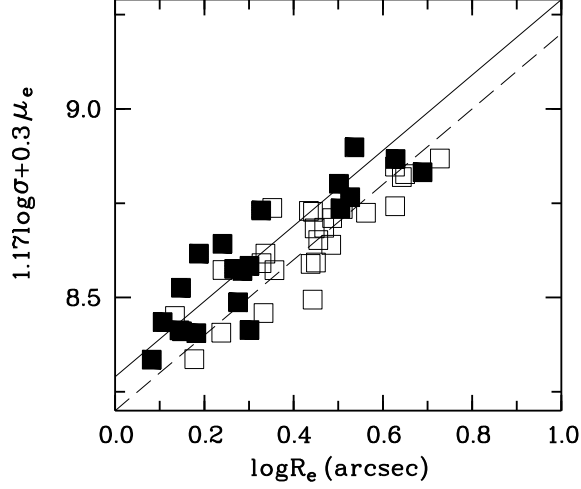


Figure 5. Fundamental plane for early-type galaxies in A1035A and A1035B (SDSS data). Designations are the same as in Fig. 4.

et al. [18] (down to the SDSS limiting magnitude of $17^m.77$). We found a total of 19 galaxies within the virialized region in each cluster. Table 2 gives the following parameters for the sample of early-type galaxies that we selected from the catalog: the J2000 equatorial coordinates; the heliocentric redshift and radial velocity; the central stellar velocity dispersion σ ; the parameters of the de Vaucouleurs profile (total magnitude and effective radius); $fracDeV_r \geq 0.8$, the quantity that characterizes the contribution of the de Vaucouleurs bulge to the surface brightness profile of the galaxy; $r_{90}/r_{50} \geq 2.6$, the concentration index, which is equal to the ratio of the radii containing 90% and 50% of the Petrosian flux, and $eClass \leq 0$, the parameter that characterizes the spectrum of the galaxy: minus means that the spectrum exhibits no appreciable emission lines.

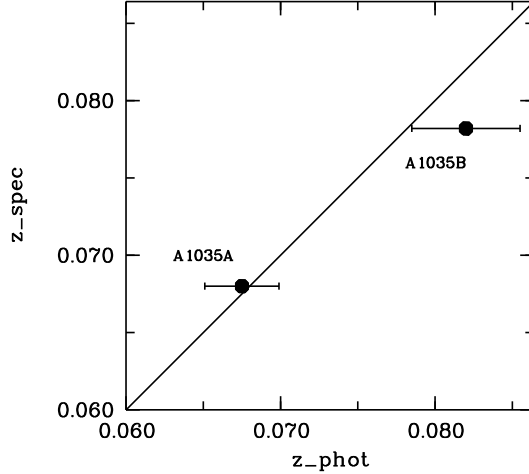


Figure 6. The Hubble diagram for A1035A and 1035B clusters. The quoted errors correspond to the error of the average distance to the cluster.

3. ANALYSIS OF RELATIVE DISTANCES OF THE SUBSYSTEMS IN A1035

Redshift-independent methods of distance determination for clusters of galaxies usually combine distance-dependent (R_e) and distance-independent (μ_e , σ) parameters of early-type galaxies. In the case of the A1035 cluster considered here, which has a bimodal distribution of radial velocities, there are two possible variants: either the A1035A and A1035B subclusters are gravitationally bound, located at the same distance, and constitute a single large cluster, or they are gravitationally unbound and obey the Hubble law, which relates radial velocity and distance, and these two subclusters are independent clusters.

A detailed description of the determination of cluster distances from the Kormendy [9] relation corrected for the dependence of residual velocities on galaxy magnitude can be found in our earlier paper [19]. The relation has the form: $\log R_e = 0.38\mu_e + \gamma$. Figure 4 (left panel) shows this relation for nine observed galaxies in A1035A and seven galaxies in A1035B. The figure gives our estimates

for the following parameters: the seeing-corrected $\log R_e$ in arcsec and the surface brightness values with cosmological correction $10 \log(1+z)$. The zero point of the relation varies with the distance to the galaxy and is assumed to be barely affected by other factors (e.g., metallicity). We find the following zero-point values with magnitude correction applied: $\gamma_A = -7.4717$ ($rms = 0.1641$), $N = 9$; $\gamma_B = -7.4633$ ($rms = 0.0474$), and $N = 7$. The zero-point difference is equal to $\gamma_{AB} = -0.008 \pm 0.058$, or, if computed without the three brightest galaxies, to $\gamma_{AB} = +0.058 \pm 0.038$. If the subsystems obey the Hubble law, then the difference of radial velocities would imply a zero-point difference of 0.061.

Photometric plane (PhP) can be derived from the fundamental plane (FP) for early-type galaxies by substituting the photometrically measurable Sersic-profile parameter for the spectroscopically measurable parameter — the central stellar velocity dispersion in the galaxy. PhP was constructed, e.g., by Graham [10]. To construct it, we use the photometric data (R_e, μ_e) [20] for 12 early-type galaxies obtained with the 6-m telescope with 200-s exposures under $1''$ seeing conditions. We determine Sersic's parameter n from the surface brightness profile.

If expressed in terms of $\log R_e$, the PhP has the following form: $\log R_e = 0.521(\pm 0.130) \log n + 0.291(\pm 0.026) \mu_e + \gamma$. Figure 4 (right panel) shows the photometric planes for the galaxies studied. We find the following zero-points for the subsystems in A1035: $\gamma_A = -5.6905$ ($rms=0.1190$), $N = 9$; $\gamma_B = -5.7878$ ($rms = 0.0710$), $N = 7$. The zero-point difference is equal to $\gamma_{AB} = +0.097 \pm 0.049$ or $\gamma_{AB} = +0.129 \pm 0.048$ if computed without the three brightest galaxies.

SDSS data for a greater number of galaxies allow the zero points (cluster distances) to be estimated more accurately, because the statistical accuracy depends on the number of galaxies. To construct the FP, we compute the mean effective surface brightness by the following formula: $\langle \mu_e \rangle = r + 2.5 \log(2\pi R_e^2) - 10 \log(1+z)$. Central velocity dispersion σ is adjusted to the standard $1/8 R_e$ circular aperture in accordance with [18]. Figure 5 shows the FP for the selected 38 galaxies with the coefficients (direct regression in terms of $\log R_e$) from Bernardi et al. [21], where it has the following form: $\log R_e = 1.17 \log \sigma + 0.30 \langle \mu_e \rangle + \gamma$. We find the following zero points for the subsystems in A1035: $\gamma_A = -8.2044$ ($rms = 0.0683$), $N = 19$; $\gamma_B = -8.2868$ ($rms = 0.0844$), and $N = 19$. The zero-point difference is equal to $\gamma_{AB} = +0.082 \pm 0.025$. The two regressions (direct and orthogonal) yield an average zero-point difference of $\gamma_{AB} = +0.076 \pm 0.026$, i.e., the distances to the two clusters differ by almost 3σ . Thus all distance-measurement methods applied show that the subsystems in the A1035 have not segregated from the Hubble flow and are independent clusters. We also determine the peculiar velocities of A1035A and A1035B in the same coordinate system as we used in our earlier paper [22] with respect to the common zero points equal to –

8.093 and -8.807 , respectively. The less distant A1035A and more distant A1035B clusters have the peculiar velocities of $+148 \pm 730 \text{ km s}^{-1}$ and $-1112 \pm 1050 \text{ km s}^{-1}$, respectively. Figure 6 shows the Hubble diagram (for the most accurate method described above) for the two clusters studied. We compute the photometric redshifts z_{phot} (0.067532 and 0.081966 for A1035A and A1035B, respectively) corresponding to our estimated cluster distance from the difference between the common zero point and the zero point of each system.

4. CONCLUSIONS

We determine the R_c -band photometric parameters (m_R , μ_e , $\log(R_e)$, n) for 16 early-type galaxies in the A1035 cluster with a bimodal distribution of radial velocities (the cluster consists of two subclusters A1035A and A1035B) from the observations made with the 1-m telescope of the Special Astrophysical Observatory of the Russian Academy of Sciences. We use these data to construct the Kormendy relation and the R_c -band photometric plane for early-type galaxies. We use SDSS (DR5) data to determine the main parameters of these clusters and construct the r -band fundamental plane for early-type galaxies. The distances to the clusters that we determine using the methods described allow us to more accurately assess the dynamical state of A1035 and determine the peculiar velocities of its subsystems. Our main conclusion is that the A1035 cluster consists of two independent systems located at their own Hubble distances. The mass of the central virialized regions is insufficient to gravitationally bind the clusters given the $\sim 3000 \text{ km s}^{-1}$ difference of their radial velocities.

ACKNOWLEDGMENTS

This work was supported in part by the Russian Foundation for Basic Research (grant no. 07-02-01417a).

This research has made use the NASA/IPAC Extragalactic Database (NED), which is operated by the Jet Propulsion Laboratory, California Institute of Technology, under contract with the NASA.

Funding for the creation and distribution of the SDSS Archive has been provided by the Alfred P. Sloan Foundation, the Participating Institutions, the National Aeronautics and Space Administration, the National Science Foundation, the US Department of Energy, the Japanese Monbukagakusho, and the Max Planck Society. The SDSS Web site is <http://www.sdss.org/>.

References

-
1. E. Hayashi, S. D. M. White, *Monthly Notices Roy. Astronom. Soc.* **370**, L38 (2006).
 2. J. R. Lucey, M. J. Currie, R. J. Dickens, *Monthly Notices Roy. Astronom. Soc.* **221**, 453 (1986).
 3. J. J. Mohr, G. Wagner, *Astronom. J.* **114**, 25 (1997).
 4. G. O. Abell, H. G. Corwin, Jr., R. P. Olowin *Astrophys. J. Suppl.* **70**, 1 (1989).
 5. M.R. Carlberg, H.K.C. Yee, E. Ellingson et al., *Astrophys. J. Suppl.* **485**, L13 (1997).
 6. K. Rines, A. Diaferio, *Astronom. J.* **132**, 1275 (2006).
 7. M. Colless, R. P. Saglia, D. Burstein et al., *Monthly Notices Roy. Astronom. Soc.* **321**, 277 (2001).
 8. M. J. Hudson, R. J. Smith, J. R. Lucey, E. Branchini, *Monthly Notices Roy. Astronom. Soc.* **352**, 61 (2004).
 9. J. Kormendy, *Astronom. and Astrophys.* **218**, 333 (1977).
 10. A. W. Graham, *Monthly Notices Roy. Astronom. Soc.* **334**, 859 (2002).
 11. S. Djorgovski, M. Davis, *Astrophys. J.* **313**, 59 (1987).
 12. A. U. Landolt, *Astronom. J.* **104**, 340 (1994).
 13. P. Grosbol. in *Reviews in modern astronomy, Springer-Verlag Berlin, Heidelberg, 1989*, Ed.: Q. Klark, **2**, 242 (2001).
 14. J. L. Sérsic, *Bol. Asoc. Argent. Astron.*, **6**, 41 (1963).
 15. G. de Vaucouleurs, *Ann. d'Astrophys.* **11**, 247 (1948).
 16. R. P. Saglia, E. Bertschinger, G. Baggley et al., *Monthly Notices Roy. Astronom. Soc.* **264**, 961 (1993).
 17. J. K. Adelman-McCarthy et al., *Astrophys. J. Suppl.*, submitted (2007).
 18. M. Bernardi, R. K. Sheth, J. Annis et al., *Astronom. J.* **125**, 1849 (2003a).
 19. F. G. Kopylova, A. I. Kopylov, *Astron. Lett.* **27**, 345 (2001).
 20. A. I. Kopylov, F. G. Kopylova, *Astronom. and Astrophys.* **382**, 389 (2002).
 21. M. Bernardi, R. K. Sheth, J. Annis et al., *Astronom. J.* **125**, 1866 (2003b).
 22. F. G. Kopylova, A. I. Kopylov, *Astron. Lett.* **33**, 211 (2007).